ELSEVIER

Chemical Engineering Journal 136 (2008) 267–275

Chemical Engineering Journal

www.elsevier.com/locate/cej

Hydroisomerization in liquid phase of a refinery naphtha stream over Pt–Ni/H-beta zeolite catalysts

Antonia Fúnez, Antonio De Lucas, Paula Sánchez*, María Jesús Ramos, José Luís Valverde

Departamento de Ingeniería Química, Facultad de Ciencias Químicas, Universidad de Castilla-La Mancha, Avd. Camilo José Cela s/n, 13071 Ciudad Real, Spain

Received 1 February 2007; received in revised form 16 March 2007; accepted 23 March 2007

Abstract

Hydroisomerization in the liquid phase of a C7–C8 stream obtained by distillation of a refinery naphtha stream using bifunctional catalysts containing Pt and/or Ni, supported on beta zeolite was studied. Temperature-programmed reduction (TPR) and temperature-programmed desorption of ammonia (TPDA) were used to characterize bimetallic interactions and the acidity of beta-supported Pt and/or Ni catalysts. Test reactions were carried out at 90 bar and 290 °C in order to achieve liquid-phase conditions.

The highest activity corresponded to the catalyst PtBETA. The addition of Pt led to a better catalytic performance at higher reaction times. Concerning the hydroisomerization products, the percentage of monobranched isomers decreased as Ni content in the catalyst increased, the contrary effect was noted for the multibranched ones. High conversion of aromatic compounds was reached. Only methylcyclopentane was obtained as a product during the hydrogenation of benzene, which implied that the presence of acid sites favoured cyclohexane isomerization to form methylcyclopentane.

Finally, an increase in the research octane number was obtained with all the catalysts due to the high amount of *iso*-paraffins and naphthenic compounds present in the products.

Keywords: Hydroisomerization; Liquid phase; Naphtha; Beta zeolite; Bimetallic catalyst; Ni–Pt

1. Introduction

Isomerization of paraffins is one of the several reactions occurring in the reforming of naphthas, which is undertaken to upgrade low octane naphtha to a higher octane effluent. Under the process conditions of reforming, other reactions could occur like aromatization (or dehydrocyclization), and dehydrogenation, with some cracking [1–3].

More severe limits on the amount of aromatics (particularly benzene) in gasoline have a negative effect on the octane number that has to be compensated by other means [3–6]. This fact has resulted in a renewed interest in the skeletal isomerization of *n*-alkanes with a view to using the branched isomers as octane-enhancing components [7]. Moreover, ring-opening reactions of aromatics compounds from reformer feedstocks are generated in isomerization reactions. For example, cyclohexane, a benzene precursor, can be rearranged over commercial paraffin isomerization catalysts to yield a mixture of branched paraffins.

The industrial processes of *n*-paraffins hydroisomerization need the presence of bifunctional catalysts. These catalysts consist in the incorporation of a noble metal on an acid support. Hydrocarbon molecules from the feed are dehydrogenated on the noble metal producing unsaturated hydrocarbons which undergo protonation on the acid centres of the support with formation of carbenium ions as reaction intermediates. These carbenium ions undergo skeletal rearrangements and β-scission reactions followed by deprotonation and hydrogenation of the resulting olefins [8–12].

Several zeolites like mordenite, USY and beta have been tested in alkane hydroisomerization [13,14]; however, the latter has a great industrial interest because its acidity and particular pore system.

As the hydrogenating–dehydrogenating function, several metals have been tested including Pt, Pd, Rh, Ir, Ru, Re

* Corresponding author. Tel.: +34 926 29 53 00; fax: +34 926 29 53 18.
E-mail address: Paula.Sanchez@uclm.es (P. Sánchez).

1385-8947/$ – see front matter © 2007 Elsevier B.V. All rights reserved.
doi:10.1016/j.cej.2007.03.062

and Ni [13]. Guisnet [15] reported the benefits that platinum produces in zeolites, because of its high resistance against the deactivation by coke. Additionally, it has been proved that catalytic performance of a metal catalyst may be influenced by the addition of a second metal [16–18]. Ward [19] reported that the property of the first dispersed metal is influenced by the addition of the second metal due to the formation of metallic clusters. Nickel was first introduced as the second metal by Vazquez et al. [20], who studied *n*-heptane isomerization and cracking over Ni–Mo/H–Y zeolite. Eswaramoorthi et al. [7] studied the hydroisomerization of *n*-hexane and *n*-heptane over Ni–Pt/HY zeolite catalysts with different Ni contents. They found that addition of Ni up to 0.3 wt.% increases the *n*-hexane and *n*-heptane conversion and multibranched isomer selectivity. Jao et al. [21] studied the isomerization of pure C_5, C_6 and C_7 feed over mordenite-supported Pt catalyst. They found that the rate of branched isomer formation was increased by adding a moderate amount of Ni. The *n*-hexane isomerization on Ni–Pt catalysts/supported on HUSY zeolite was studied by Yoshioka et al. [6]. Bimetallic Ni–Pt catalysts showed to have smaller deactivation and much higher activity compared to monometallic Ni catalysts. They also observed that the selectivity for the production of di-ramified alkanes increases as the Ni content does.

Concerning the feed used in the hydroisomerization reactions, most of the research efforts have been made over hydrocarbon mixtures, mainly binary and ternary ones [11,12]. Jiménez et al. [12] studied the hydroisomerization of a hydrocarbon feed containing *n*-hexane, *n*-heptane and cyclohexane over zeolite catalysts. Gopal et al. [11] reported the hydroisomerization of C5–C7 alkanes and simultaneous saturation of benzene over Pt/H-ZSM-12 and Pt/BETA. However, until now the hydroisomerization of a real naphtha stream has been scarcely studied [2].

On the other hand, most of studies on hydroisomerization have been performed in vapour phase using a hydrogen pressure below 10 bar [22,23], being very scarce the existing literature about this process in liquid phase.

In this work the liquid-phase hydroisomerization of a C7–C8 fraction obtained by distillation of a real naphtha stream on beta-based catalysts, containing both platinum and/or nickel was studied. Most of studies using bimetallic catalysts are performed with catalysts having a constant mass, which can lead to wrong readings because the atomic weight of both metals is different [6]. In this study, catalysts containing a constant metal molar concentration will be compared. A pressure of 90 bar was enough to achieve liquid-phase conditions at a temperature of 290 °C.

2. Experimental

2.1. Catalyst preparation

The bifunctional catalysts used in this work consisted of H-Beta as the acid function and Pt and/or Ni as the metal function. Beta zeolite (Si/Al = 13.0) was supplied in the ammonium form by Zeolyst International. Calcination at 550 °C for 15 h yielded the acid form of the zeolite.

Table 1
Metal loading of the catalysts

Catalyst	Composition of the metal phase (mol%)		Metal loading (wt.%)		
	Pt	Ni	Pt	Ni	Total
PtBETA	100	0	1.00	0.00	1.00
0.75Pt0.25NiBETA	75	25	0.86	0.09	0.94
0.50Pt0.50NiBETA	50	50	0.57	0.17	0.74
0.25Pt0.75NiBETA	25	75	0.29	0.26	0.54
NiBETA	0	100	0.00	0.34	0.34

Metal incorporation was carried out by an impregnation technique. The metallic composition of the samples is compiled in Table 1. The total metal loading was kept constant at 0.058 mmol metal per gram of zeolite. The total weight (%) corresponding to the metal loading varied between 1 and 0.34. The sample was placed in a glass vessel and kept under vacuum at room temperature for 2 h in order to remove water and other compounds adsorbed on the zeolite. A known volume of an aqueous metal precursor solution was then poured over the zeolite. As metal precursor, H_2PtCl_6 or $Ni(NO_3)_2$ were used. These compounds are commonly reported in the literature [6,13,21]. Next, the solvent was removed by evaporation under vacuum. The metal content added to the catalyst was controlled by measuring the metal concentration in the impregnating solution. In the case of bimetallic catalysts, a simultaneous impregnation with both precursors was employed. After metal incorporation, the catalysts were calcined at 400 °C for 4 h and reduced in situ under a hydrogen flow of 190 ml min^{-1} g^{-1}.

The monometallic samples were named to as PtBETA and NiBETA, whereas bimetallic samples were identified as follows: first, the relative metal molar percentage of the metal phase (0.25, 0.50, and 0.75 g) was indicated; second, the metal (Pt or Ni) was considered, and, finally, the name of the zeolite (BETA) was included.

2.2. Catalyst characterization

BET surface area was determined by nitrogen adsorption and desorption data acquired on a Micromeritics ASAP 2010 apparatus. The sample was pretreated overnight at 350 °C under vacuum of 5×10^{-3} Torr at 350 °C for 15 h. Specific total surface areas were calculated using the BET equation. Surface area measurements had an error of ±3%.

In order to quantify the real amount of metal incorporated in the catalyst, atomic absorption (AA) measurements were performance using a SpectrAA 220FS spectrophotometer. The error of these measurements was below 1%.

The concentration of the acid sites was measured by temperature-programmed desorption of ammonia (TPDA) using a Micromeritics TPD/TPR 2900 analyzer. The sample was firstly heated from room temperature to the calcination temperature at 15 °C min^{-1} under a flow of helium, holding this temperature during 30 min. After reducing the catalysts under a hydrogen

flow, the system was cooled to 180 °C. Ammonia was then flowed over the sample for 15 min. Later, the sample was purged with helium for 1 h in order to eliminate physisorbed species. The temperature was ramped at 15 °C min^{-1} from 180 to 560 °C and TPDA data were acquired. The total acidity was obtained by integration of the area under the curve. Weak and strong acidities are defined as the concentration of weak and strong acid sites, respectively, obtained by integration of the area under the peaks at the lowest and the highest temperatures, respectively [24,25].

TPR measurements were carried out with the same apparatus described above (Micromeritics TPD/TPR 2900 analyzer). After loading, the sample was outgassed by heating at 20 °C min^{-1} in an argon flow up to the calcination temperature of the sample and kept constant at this temperature for 30 min. Next, it was cooled to room temperature and stabilized under an argon/hydrogen flow (≥99.9990% purity, 85/15 volumetric ratio). The temperature and detector signals were then continuously recorded while heating at 20 °C min^{-1} up to 800 °C. The liquids formed during the reduction process were retained by a cooling trap placed between the sample and the detector. TPR profiles were reproducible, standard deviations for the temperature of the peak maxima being ±2%. The TPR profiles were fitted to several peaks by Gaussian deconvolution trying to keep the peak maxima constant.

2.3. Distillation procedure

A naphtha stream (containing *n*-paraffins, isoparaffins, aromatics and naphthenes) supplied by the company REPSOL-YPF (from Spain) was the feed to a pilot plant distillation unit. The naphtha stream composition and the distillation unit scheme were depicted elsewhere [2]. In order to define a specific stream to be fed to the reactor, a distillation process was carried out. It was obtained three main fractions: C5–C6 and C7–C8 fractions (the latter with a molar content of C6 compounds lower than 4.6%) and a third one consisting of hydrocarbons with a carbon number equal or higher than 9. In order to estimate the boiling temperature of each fraction, a HYSYS application (supplied by AspenTech) was developed. Thus, the distillation temperatures of each of the three fractions were: 59–98, 98–127 and >127 °C, respectively. The corresponding ASTM curve calculated using HYSYS was shown elsewhere [3].

The batch distillation procedure was as follows: the naphtha stream was placed in the reboiler. The temperature was increased to reach the boiling point of the liquid feed. At first, all the vapour phase was condensed and returned to the column. Once the steady state was achieved, a liquid phase was obtained as the distillate (reflux ratio of 0.4). The composition of the C7–C8 fraction, obtained by distillation of the refinery naphtha stream, is given in Table 2.

Table 2
Molar composition of the C7–C8 distillated stream (feed)

Carbon atoms	Molar composition (%)				
	n-Paraffins	*iso*-Paraffins	Naphthenes	Aromatics	Total
6	2.47	0.71	1.30	2.85	4.57
7	14.50	12.44	20.47	0.10	50.26
8	7.12	29.19	8.86	0.00	45.17

2.4. Catalytic experiments

The C7–C8 fraction hydroisomerization reactions were carried out in a 50 ml batch microreactor (Autoclave Engineers). Firstly, the catalyst was reduced in a fixed-bed reactor under a hydrogen flow of 190 ml min^{-1} g^{-1} at 410 °C for 4 h.

Consequently, the batch microreactor was filled with 17 ml of the feed and the catalytic basket with 0.75 g of catalyst. Afterwards, it was pressurized at 80 bar with hydrogen and heated gradually at 290 °C. Once this temperature was reached, the total pressure was finally set at 90 bar. It was experimentally verified that a stirring rate over 370 rpm was sufficient to establish complete mixing in the reactor. Blank runs demonstrated that *n*-paraffins conversion was negligible. The reaction time was elapsed up to 24 h. Samples (20 μl) of the vapour and liquid products were taken at regular intervals. Gas products were analyzed in a gas chromatograph (HP 5890 Series II) equipped with a flame ionization detector and a capillary column (SUPELCO Petrocol DH 50.2, 0.2 mm i.d. and 50 m length). Liquid products were analyzed in a gas chromatograph (GC-17A SHIMADZU) coupled to a mass spectrometer (QP-5000 SHIMADZU). A capillary column (SUPELCO Petrocol DH, 100-m length with a 0.25 mm internal diameter) was used in this GC.

Results from a reproduced experiment showed that conversion and isomer selectivity had an error of ±3%.

3. Results and discussion

3.1. Catalysts characterization

The characterization data of the catalysts used in this work are summarized in Table 3.

Table 3
Surface area and acidity data values of the catalysts

Catalyst	Surface area (m^2 g$_{cat}^{-1}$)	Total acidity (mmol NH_3 g$_{cat}^{-1}$)	Weak acidity (mmol NH_3 g$_{cat}^{-1}$)	Strong acidity (mmol NH_3 g$_{cat}^{-1}$)
PtBETA	614	0.799	0.187	0.612
0.75Pt0.25NiBETA	594	0.779	0.180	0.599
0.50Pt0.50NiBETA	589	0.744	0.175	0.569
0.25Pt0.75NiBETA	578	0.678	0.188	0.490
NiBETA	583	0.718	0.172	0.546

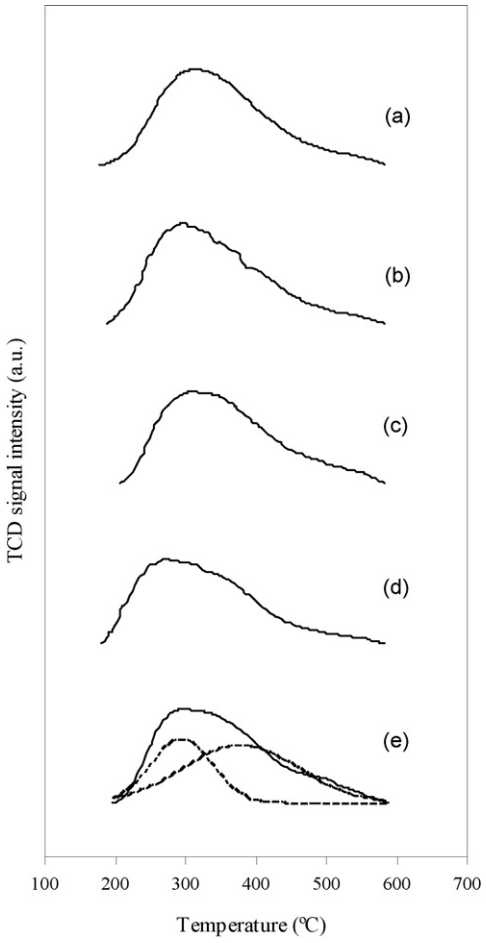

Fig. 1. NH_3 TPD profiles for the catalysts: (a) PtBETA, (b) 0.75Pt0.25NiBETA, (c) 0.50Pt0.50NiBETA, (d) 0.25Pt0.75NiBETA and (e) NiBETA (dotted lines represent deconvolution).

TPD profiles characterizing NH_3 adsorbed on the different catalysts are shown in Fig. 1. Peak position did not vary substantially with the different metal concentration combination. In all cases, the desorption curves were deconvoluted and fitted to two peaks, whose maximum temperatures were nearly 300 and 370 °C. These two peaks corresponded to the desorption of ammonia on weak and strong acid sites, respectively. The amount of ammonia desorbed and the desorption temperature were considered as a measure of total acidity and acid strength of catalysts, respectively [26]. It is observed from Table 3 that the amount of ammonia adsorbed at higher temperature (strong acidity) was always found to be greater than that adsorbed at lower temperature (weak acidity). Furthermore, an increase of Ni loading led to a decrease of the total acidity of the bimetallic catalysts. The decrease in acidity of the bimetallic catalysts with higher nickel loadings can be accounted for in terms of occupation of some acid sites by added nickel species [7,21,27]. This process may occur in parallel with Ni combining with Pt particles and the probable growth of Ni–Pt particles [7]. As shown in Table 3, a slight decrease in the values of the surface area with increasing Ni loading was also observed. This fact suggests that there would not be a significative blocking of zeolite channels by the nickel species. However, it is not possible to claim that a partial blocking of the zeolite micropore mouths by these species occurred because the surface area measurements were evaluated by using a small molecule like N_2 [14]. Some authors [28] found a lower acid site density and surface area when Ni was introduced in mordenite zeolite and also suggested a partial pore blockage by the Ni particles.

On the other hand, the maximum temperature corresponding to the ammonium desorption profile was not significantly affected by an increase of Ni loading. This would indicate that the Ni content did not affect the strength of acid sites (Fig. 1) [21].

Temperature-programmed reductions were carried out in order to determine the relative differences in the reducibility of the catalysts impregnated with different metal loadings. TPR profiles of monometallic catalysts (Pt or Ni/BETA) and bimetallic catalysts (Pt–Ni/BETA) are shown in Fig. 2. Two reduction peaks at 400 and 610 °C, respectively, were detected for the sample NiBETA. The peak at 400 °C could be related to the reduction of NiO to Ni^0 [28]. It is very likely that some Ni^{2+} to be ion-exchanged during the impregnation process [28]. It is also possible that part of the NiO particles formed during the calcinations of these catalysts to react with protons of the zeolite to form $Ni(OH)^+$. The second peak at 610 °C was due to the reduction of stabilized Ni^{2+} species located into zeolite sites, where

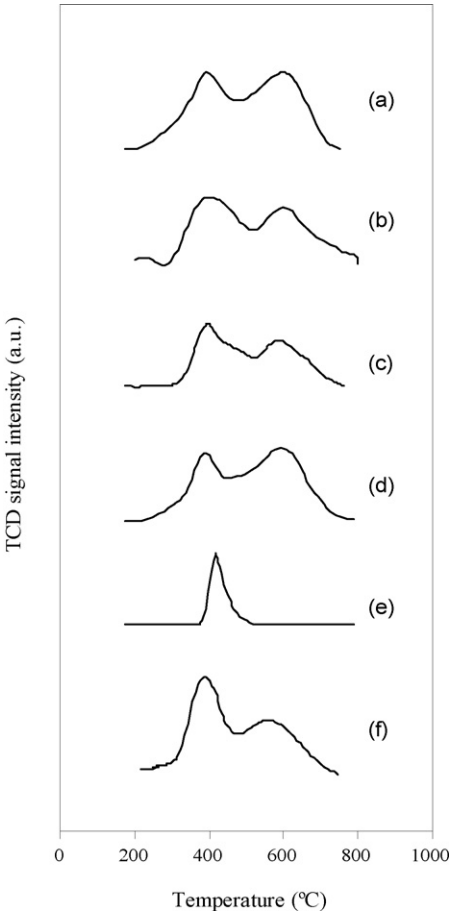

Fig. 2. TPR profiles for the catalysts: (a) NiBETA, (b) 0.25Pt0.75NiBETA, (c) 0.50Pt0.50NiBETA, (d) 0.75Pt0.25NiBETA, (e) PtBETA and (f) a physical mixture of PtBETA and NiBETA.

the access for H_2 molecules should be difficult [6]. Moreover, these ions located in small cavities could strongly interact with the zeolite structure in order to form less reducible species.

However, in the case of the sample PtBETA, only one peak at 390 °C, which may be attributed to the reduction of Pt^{2+} to Pt^0 [25], was detected.

On the other hand, it can be clearly appreciated two reduction peaks for all the bimetallic catalysts. The first peak (400 °C) corresponds to the reduction of NiO and Pt^{2+} species and the second peak to the reduction of stabilized Ni^{2+} species. Some authors observed for bimetallic Ni–Pt catalysts only a single TPR peak. Jao et al. [21] found only a maximum for a Ni(0.5)–Pt(0.26) mordenite catalyst. Raab et al. [29] also observed only a sharp maximum in the TPR profile for the silica-supported Ni–Pt catalysts with a Pt concentration in the metallic phase greater than 50 mol%. This fact may indicate a catalytic reduction of Ni by prereduced Pt particles [21], what suggests the formation of Ni–Pt bimetallic interactions. Our results suggest that segregate Ni and Pt particles were mainly formed on the zeolite surface [21], although it may also be possible physical Ni–Pt bimetallic interactions. As shown in Fig. 2, TPR of a physical mixture of samples PtBETA and NiBETA showed that both Ni and Pt species were reduced separately. The maximum reduction rate of Ni and Pt in bimetallic catalysts exhibited no significant change compared to those corresponding to the summation of TPR spectra characterizing the monometallic samples. This fact would support the picture of segregate metallic particles over the bimetallic catalysts. Anyway, the existence in these samples of Ni–Pt particles should not be totally neglected.

3.2. Hydroisomerization of the C7–C8 fraction

3.2.1. Paraffins conversion

Fig. 3 shows the overall paraffins conversion, defined as the conversion of linear hydrocarbons (i.e., conversion of *n*-heptane and *n*-octane) versus the reaction time for the different catalysts used in this work. Thermal conversion of the C7–C8 distillated stream was always below 1% and, hence, can be neglected at the experimental conditions used. It can be seen that at short reaction times the monometallic catalysts (PtBETA and NiBETA) showed the highest activity. When the reaction time increased, the bimetallic catalysts exhibited better catalytic performance than the catalyst containing only Ni. This fact implies that at higher reaction times the addition of Pt significantly increased the catalyst activity. This behaviour can be explained attending to the acid site density of the catalyst, which affected to the paraffins conversion [30,31]; specifically, strong acid sites were the responsible of the isomerization reaction [32]. As above mentioned, the acidity values for the catalysts lowered as the nickel content was increased. A partial blocking of the micropores of the zeolite by the Ni particles could take place, which could hinder the access to the acid sites. This behaviour is supported by the fact that surface area measured (Table 3) slightly decreased with increasing Ni loading.

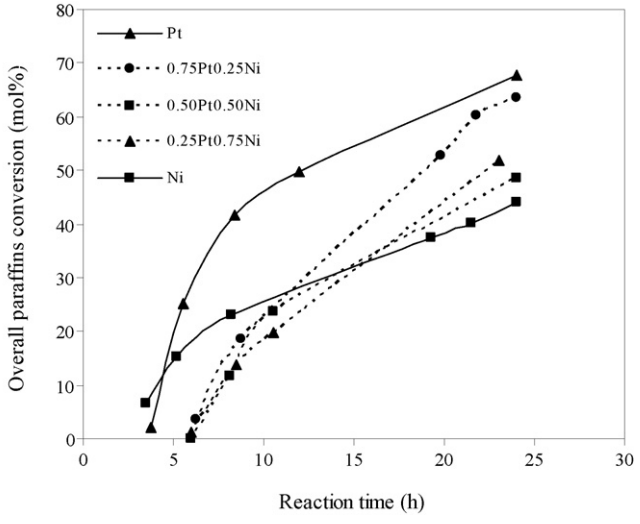

Fig. 3. Overall paraffins conversion (mol%) vs. the reaction time for all the catalysts.

On the other hand, as the isomerization mechanism predicts, alkane transformation occurs through successive steps [33]. First, the alkane is dehydrogenated on the metal site and, then, the olefins formed are transported to the acid sites. The hydroisomerization reaction is considered ideal when the metal component is present in sufficient excess amount, to consider that the reactions in the acid sites to be the rate-limiting step [34]. If the available metallic sites are not sufficient for all the acid sites to be fed with intermediate alkenes, the activity per acid site will decrease. There are a large number of strong acid sites available on HBETA [31], so, the metallic sites became the limiting factor to the degree of a catalyst activity [6].

The initial activity of the Ni catalyst was higher than that of the Pt–Ni catalysts, whereas lower conversion was obtained at higher reaction times. These results indicate that the Ni catalyst underwent a more rapid deactivation than the bimetallic ones. Similar results were reported by other authors [21].

Moreover, it is clear that the high activity and selectivity exhibited by the platinum catalyst was due not only to the high dispersion but also to its great hydrogenating–dehydrogenating capacity in hydroisomerization processes [10,14,32].

3.2.2. Branched products

The molar product distribution, at approximately 40 mol% of overall paraffins conversion, is given in Table 4. Regardless the catalysts, the same kind of products were obtained, which included C1–C6 hydrocarbons (considered as cracking products obtained from β-scissions of C7 and C8 hydrocarbons), products with 7–8 carbon atoms (monobranched, dibranched and tribranched isomers and the corresponding linear paraffins), naphthenic and aromatics compounds. C9 or higher products were not observed.

The absence of methane and ethane revealed that hydrogenolysis did not contribute to the cracking reaction [3].

Since the purpose of the hydroisomerization process is to achieve an increase in the octane number of the gasoline, it is interesting to note the formation of multibranched isomers from the C7–C8 distillated stream used as the feed, because multibranched isomers have higher octane ratings. As shown in

Table 4
Composition (mol%), at approximately 40 mol% of overall paraffins conversion, for the products obtained in the hydroisomerization of the C7–C8 distillated stream catalyzed by beta-supported Pt/Ni catalysts

Catalyst Reaction time (h)	Feed	PtBETA (8.5)	0.75Pt0.25Ni (20.0)	0.50Pt0.50Ni (24.0)	0.25Pt0.75Ni (23.0)	NiBETA (21.5)
C1 + C2	0.00	0.00	0.00	0.00	0.00	0.00
C3	0.00	0.00	0.00	0.00	0.00	0.91
iso-C4	0.00	2.83	3.26	3.38	5.34	5.53
n-C4	0.00	0.85	0.00	0.00	1.53	1.47
iso-C5	0.00	2.21	2.35	2.71	4.47	6.03
n-C5	0.00	0.00	0.00	0.00	0.00	1.28
2,3-DMC4	0.00	0.00	0.00	0.00	0.00	1.13
2-MC5	0.34	1.02	0.95	0.00	1.50	3.94
3-MC5	0.37	0.00	0.00	0.00	0.00	2.42
n-C6	2.47	1.74	1.57	1.44	1.58	2.35
2,2-DMC5	0.00	1.88	0.00	1.40	0.94	0.55
2,4-DMC5	0.00	2.07	2.50	2.04	1.80	1.92
2,2,3-TMC4	0.00	0.00	0.00	0.00	0.00	0.00
3,3-DMC5	0.00	0.00	0.00	0.00	0.00	0.65
2-MC6	4.45	8.74	8.16	8.38	7.32	6.78
2,3-DMC5	1.54	2.85	2.94	3.85	3.09	3.54
3-MC6	5.84	9.38	8.91	9.13	8.06	8.37
3-EC5	0.61	0.00	0.00	0.00	0.00	1.05
n-C7	14.50	8.97	9.18	6.78	7.05	9.20
2,2-DMC6	1.42	1.49	0.94	1.20	1.08	1.21
2,5-DMC6	1.24	2.07	1.89	3.55	0.75	1.07
2,4-DMC6	1.86	2.93	2.25	2.53	0.65	0.80
3,3-DMC6	1.86	0.00	1.50	1.42	2.12	1.45
2,3,4-TMC5	2.01	0.00	0.00	0.00	1.38	3.18
2-M-3-EC5	1.07	0.00	0.00	0.00	0.94	1.13
2,3-DMC6	1.34	0.00	0.87	0.00	0.73	0.44
2-MC7	8.18	5.74	5.30	5.06	2.59	1.41
4-MC7	2.85	2.37	4.33	2.16	1.38	1.55
3,4-DMC6	1.98	0.00	0.54	0.00	0.97	0.00
3-MC7	5.02	5.43	5.12	4.82	2.06	2.00
3-EC6	1.84	0.00	1.60	0.00	0.00	1.73
n-C8	7.12	3.33	0.66	4.19	3.02	2.01
Monobranched (mol%)	28.19	31.66	33.42	29.55	21.39	22.89
Multibranched (mol%)	13.43	13.29	13.43	15.96	14.45	15.99
Naphthenes						
MCP (methylcyclopentane)	1.40	3.68	3.49	3.53	4.68	2.86
CH (cyclohexane)	1.12	0.00	0.00	0.00	0.00	0.00
MCH (methylcyclohexane)	12.82	12.69	13.13	12.98	16.66	5.61
DMCPs (dimethylcyclopentanes)[a]	6.45	13.01	14.46	13.91	14.81	11.76
ECP (ethylcyclopentane)	1.21	2.09	2.06	1.01	0.98	0.65
TMCPs (trimethylciclopentanes)[b]	3.24	0.10	0.08	0.41	0.00	0.00
DMCHs (dimethylciclohexanes)[c]	5.45	1.73	1.85	2.58	2.30	2.72
Aromatics						
Benzene	2.83	0.00	0.00	0.00	0.00	0.98
Toluene	1.65	0.00	0.00	0.00	0.00	0.00

[a] DMCP = 1,1-dimethylcyclopentane, 1,2-*trans*-dimethylcyclopentane, 1,3-*trans*-dimethylcyclopentane, 1,2-*cis*-dimethylcyclopentane, 1,3-*cis*-dimethylcyclopentane.
[b] TMCP = 1-*trans*-2-*cis*-4-trimethylcyclopentane, *cis*-*trans*-*cis*-1-2-3-trimethylcyclopentane.
[c] DMCH = *cis*-1,3-dimethylcyclohexane, *trans*-1,4-dimethylcyclohexane, *trans*-3-ethylcyclopentane, *cis*-3-ethylcyclopentane, *trans*-2-ethylcyclopentane, 1-ethyl-1-methylcyclopentane, *trans*-1,2-dimethylcyclohexane.

Fig. 4, at lower conversions, the monobranched isomers were predominant over PtBETA. They were clearly primary products of the reaction. When the reaction time increased, and then, the conversion, the monobranched selectivity decreased. The multibranched selectivity firstly increased with the conversion, then passed through a maximum and finally decreased. Cracked products appeared at higher conversions values. The same trend was obtained for the rest of catalysts.

The percentage of mono and multibranched paraffins in the feed was 28.19 and 13.43, respectively. In Table 4 it is also displayed the molar percentage of mono and multibranched isomers obtained with each catalyst at approximately 40 mol% of overall paraffins conversion. In general, it can be appreciated a lower percentage of monobranched isomers for the catalysts containing Ni; the opposite effect being detected for multibranched isomers. Jao et al. [21] observed that the addition of

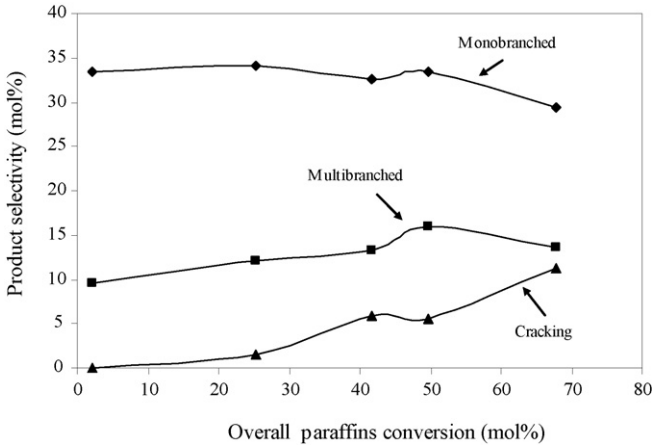

Fig. 4. Products selectivity versus overall conversion paraffins over catalyst PtBETA.

a moderate amount of Ni (from 0.2 to 0.5 wt.%) to Pt/HMOR enhanced the rate of branched isomer formation. Yoshioka et al. [6] observed an increase in the formation of di-ramified isomers for the monometallic catalysts that contained Ni.

Recently, our research group [2,3] has reported the hydroisomerization of a C7–C8 stream feedstock in vapour phase using catalysts based in palladium and platinum containing zeolites. It is worth noting that the percentage of isoparaffins obtained in vapour phase was always lower than that obtained in liquid phase. These results agree with those reported by Denayer et al. [22]. These authors observed that due to the high pressure used in the liquid-phase reaction, the cracking products formation became only important at relatively high average conversions.

3.2.3. Aromatic and naphthenic compounds

As can be seen in Table 4, benzene and toluene were only detected in the feed. Benzene and aromatics compounds are known to have a substantial impact on health. Environmental concerns have promoted legislation to limit the amount of total aromatics, and, particularly benzene, in gasoline [4,11]. The limits imposed for benzene and aromatic compounds are 1 and 35 vol.%, respectively. All the catalysts used in this work (except NiBETA) reached a total conversion of aromatic compounds. A conversion of 65.5 mol% of benzene was obtained with the sample NiBETA.

The molar composition of the naphthenic compounds in the feed and in the products obtained with each catalyst is also shown in Table 4. Methylcyclopentane (MCP) and cyclohexane (CH) are the typical products obtained during the hydrogenation of benzene over bifunctional catalysts [4,11,35]. However, only MCP was obtained as a product, which implies that the benzene hydrogenation led to the formation of CH, which in presence of acid sites produced MCP by isomerization [35]. These results are according to the thermodynamic equilibrium, which predicts that MCP is produced in higher quantities during the hydroisomerization [11].

On the other hand, methylcyclohexane (MCH) was obtained by toluene hydrogenation [36,37]. The rearrangement of MCH in terms of isomerization reactions led to dimethyl (1,1-, 1,2-*cis* and -*trans* and 1,3-*cis* and -*trans*) and ethyl-cyclopentanes (DMCP and ECP, respectively). Isomerization of MCH to both DMCP and ECP is supposed to take place on the acid sites of the zeolite while the hydrogenation of toluene is performed by a metal function [38]. The MCH composition in the product was similar to that of the feed, except for sample NiBETA. A lower MCH concentration was obtained with this catalyst. However, a great increase in the DMCP concentration was obtained with all catalysts (Table 4). This fact proved that once the toluene was hydrogenated into MCH, this compound underwent skeletal rearrangements reactions leading to different DMCP compounds.

MCH and DMCP concentration was significantly higher when catalyst 0.25Pt0.75NiBETA was used. These naphthenic compounds would contribute to an increase of the octane number of the product. The lower concentration of MCH and DMCP obtained with sample NiBETA would indicate the occurrence of ring-openings reactions. As a consequence, branched C7 hydrocarbons could undergo successive cracking reactions, yielding mainly C3 and C4 hydrocarbons.

Other naphthenic compounds like trimethylcyclopentanes (TMCP) and dimethylcyclohexanes (DMCH) were detected as final products. However, their concentration was lower as that observed in the feed (Table 4). The contribution of the ring-opening reactions to the disappearance of these compounds led to the formation of branched octane isomers [39], which underwent cracking reactions when the conversion level increased.

It is worthy to note that at 40 mol% of overall paraffins conversion, the presence of branched octane isomers can be due to both the isomerization of *n*-octane and the contribution of the ring-opening reactions of TMCP and DMCH.

3.3. Research octane number

Because the aim of the hydroisomerization process is to achieve an increase in the octane number of the gasoline, it is interesting to compare the increase of the RON when the feed was converted using different catalysts. For this purpose, the research octane number of the C5+ fraction in the product was estimated. The RON of the mixture was evaluated as the product of the volume fraction of the individual C5 and higher hydrocarbons and their corresponding RON, then summing up the contributions of all the compounds [11]. This procedure was also used to estimate the research octane number of the feed. It resulted to be 47.18.

In practice, octane numbers do not blend linearly. To accommodate this, complex blending calculations employing blending octane numbers as opposed to the values for pure hydrocarbons are routinely employed. In general, the blending octane numbers are greater than the corresponding pure octane numbers; e.g., MCP has a higher estimated research octane number than CH, but the blending octane numbers of both MCP and CH are similar. This method for estimating RON values of mixtures is likely to be different from that used to calculate the real RON value, the latter being generally higher [11].

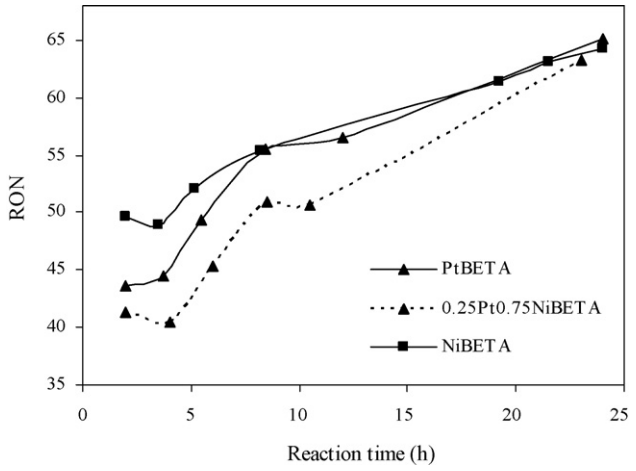

Fig. 5. RON value as a function of the reaction time over monometallic and 0.25Pt0.75NiBETA samples.

Fig. 5 includes the evolution of RON values with the reaction time for the monometallic catalysts and one bimetallic sample (0.25Pt0.75NiBETA). Similar trends were showed for the rest of bimetallic catalysts. It can be clearly seen that the catalysts performed a good hydroisomerization reaction. In all cases, RON was increased significantly. The increase in the octane number when sample 0.25Pt0.75NiBETA was used was fundamentally due to the increase in the content of naphthenic compounds (MCH and DMCP). Sample NiBETA yielded a higher amount of multibranched isomers which led to higher RON values than those corresponding to linear alkanes. This increase in the RON value was also due to the contribution of not converted benzene present in the product.

4. Conclusions

The hydroisomerization in liquid phase of a C7–C8 stream obtained by distillation of a real naphtha stream was carried out using bifunctional Pt–Ni-Beta zeolite catalysts.

The overall paraffins conversion was defined as the conversion of linear hydrocarbons. The highest overall conversion was obtained with the catalyst containing only Pt. At higher reaction times, the bimetallic catalysts showed a catalytic activity higher than the catalyst containing only Ni.

The same types of products were obtained with all the catalysts, including C1–C6 hydrocarbon (considered as cracking products obtained from the β-scission of C7 and C8 hydrocarbons), products with 7–8 carbon atoms (mono and multibranched), naphthenes and aromatic compounds.

An increase in the percentage of multibranched isomers was detected when the Ni content increased in the catalysts, the contrary effect was noted for the monobranched content.

All the catalysts used in this work, but NiBETA, led to a total removal of aromatic compounds. A conversion of 65.5 mol% of benzene was achieved with sample NiBETA.

An increase in the RON value was detected for all the catalysts. The increase in RON value for bimetallic sample 0.25Pt0.75NiBETA was due to the increase in the content of naphthenic compounds (MCH and DMCP) in the product. Sample NiBETA yielded a higher amount of multibranched isomers which contributed to high RON values.

Acknowledgements

Financial support from Ministerio de Ciencia y Tecnología of Spain (ProjectCTQ-2004-07350-C02-O) and Consejería de Ciencia y Tecnología de la Junta de Comunidades de Castilla-La Mancha (Proyect PBI-05-038) are gratefully acknowledged.

References

[1] A. Huss, M.N. Harandi, D.J. Esteves, D.J. Dovedytis, K.J. Del Rossi. U.S. Patent 5,334,792 (1994).
[2] M.J. Ramos, J.P. Gómez, A. De Lucas, F. Dorado, P. Sánchez, J.L. Valverde, Ind. Eng. Chem. Res. 44 (2005) 9050–9058.
[3] M.J. Ramos, J.P. Gómez, A. De Lucas, F. Dorado, P. Sánchez, J.L. Valverde, Chem. Eng. J., in press.
[4] M.A. Arribas, F. Márquez, A. Martínez, J. Catal. 190 (2000) 309–319.
[5] J.M. Serra, A. Chica, A. Corma, Appl. Catal. A: Gen. 239 (2003) 35–42.
[6] C.M.N. Yoshioka, T. Garetto, D. Cardoso, Catal. Today 107–108 (2005) 693–698.
[7] I. Eswaramoorthi, N. Lingappan, Catal. Lett. 87 (2003) 133–142.
[8] J.A. Muñoz, G.G. Martens, G.F. Froment, G.B. Marin, P.A. Jacobs, J.A. Martens, Appl. Catal. A: Gen. 192 (2000) 9–22.
[9] A. De Lucas, J.L. Valverde, P. Sánchez, F. Dorado, M.J. Ramos, Ind. Eng. Chem Res. 43 (2004) 8217–8225.
[10] A. De Lucas, J.L. Valverde, P. Sánchez, F. Dorado, M.J. Ramos, Appl. Catal. A: Gen. 282 (2005) 15–24.
[11] S. Gopal, P.G. Smirniotis, Appl. Catal. A: Gen. 247 (2003) 113–123.
[12] C. Jiménez, F.J. Romero, R. Roldán, J.M. Marinas, J.P. Gómez, Appl. Catal. A: Gen. 249 (2003) 175–185.
[13] A. De Lucas, P. Sánchez, A. Fúnez, M.J. Ramos, J.L. Valverde, J. Mol. Catal. 259 (2006) 259–266.
[14] A. De Lucas, P. Sánchez, A. Fúnez, M.J. Ramos, J.L. Valverde, Ind. Eng. Chem. Res., in press.
[15] M. Guisnet, Polish J. Chem. 77 (2003) 637–656.
[16] J.-K. Lee, H.-K. Rhee, J. Catal. 177 (1998) 208–216.
[17] L.I. Ali, A.-G.A. Ali, S.M. Aboul-Fotouh, A.K. Aboul-Gheit, Appl. Catal. A: Gen. 205 (2001) 129–146.
[18] A. De Lucas, P. Sánchez, F. Dorado, M.J. Ramos, J.L. Valverde, Appl. Catal. A: Gen. 294 (2005) 215–225.
[19] J.W. Ward, Fuel Process. Technol. 32 (1993) 55–85.
[20] I.M. Vazquez, A. Escardino, A. Corma, Ind. Eng. Chem. Res. 26 (1987) 1495–1500.
[21] R.M. Jao, T.B. Lin, J.R. Chang, J. Catal. 161 (1996) 222–229.
[22] J.F.M. Denayer, R.A. Ocakoglu, W. Hybrechts, B. Dejonckheere, P. Jacobs, S. Calero, R. Krishna, B. Smit, G.B. Baron, J.A. Martens, J. Catal. 220 (2003) 66–73.
[23] T.D. Pope, J.F. Kriz, M. Stanciulescu, J. Monnier, Appl. Catal. A: Gen. 233 (2002) 45–62.
[24] F. Dorado, R. Romero, P. Cañizares, Appl. Catal. A: Gen. 236 (2002) 235–243.
[25] P. Cañizares, A. De Lucas, J.L. Valverde, F. Dorado, Ind. Eng. Chem. Res. 36 (1997) 4797–4808.
[26] L.J. Leu, L.Y. Hou, B.C. Kang, C. Li, S.T. Wu, J.C. Wu, Appl. Catal. A: Gen. 69 (1991) 49–63.
[27] I. Eswaramoorthi, N. Lingappan, Korean J. Chem. Eng. 20 (2) (2003) 133–142.
[28] P. Cañizares, A. De Lucas, F. Dorado, A. Durán, I. Asencio, Appl. Catal. A: Gen. 169 (1998) 137–150.
[29] C. Raab, J.A. Lercher, J.G. Goodwin, J.Z. Shyu, J. Catal. 122 (1990) 406–414.
[30] G. Kinger, H. Vinek, Appl. Catal. A: Gen. 218 (2001) 139–150.
[31] K. Park, S. Ihm, Appl. Catal. A: Gen. 203 (2000) 201–209.

[32] W. Zhang, P.G. Smirniotis, J. Catal. 182 (1999) 400–416.
[33] P.B. Weisz, Adv. Catal. 13 (1962) 137–190.
[34] J.W. Thybaut, C.S.L. Narasimhan, J.F. Denayer, G.V. Baron, P.A. Jacobs, J.A. Martens, G.B. Marin, Ind. Eng. Chem. Res. 44 (2005) 5159–5169.
[35] L.J. Simon, J.G. van Ommen, A. Jentys, J.A. Lercher, J. Catal. 203 (2001) 434–442.
[36] T. Osaki, T. Tanaka, Y. Tai, Phys. Chem. Chem. Phys. 1 (1999) 2361–2366.
[37] M.S. Lylykangas, P.A. Rautanen, A.O.I. Krause, Ind. Eng. Chem. Res. 41 (2002) 5632–5639.
[38] H. Belatel, H. Al-Kandari, F. Al-Khorafi, A. Katrib, F. Garin, Appl. Catal. A: Gen. 275 (2004) 141–147.
[39] G.B. McVicker, M. Daage, M.S. Touvelle, C.W. Hudson, D.P. Klein, W.C. Baird Jr., B.R. Cook, J.G. Chen, S. Hantzer, D.E.W. Vaughan, E.S. Ellis, O.C.S. Feeley, J Catal. 210 (2002) 137–148.